Structure and magnetic properties of the $S=1$ geometrically frustrated double perovskites La_2LiReO_6 and Ba_2YReO_6

Tomoko Aharen,[1] John E. Greedan,[1,2] Craig A. Bridges,[1] Adam A. Aczel,[3] Jose Rodriguez,[3] Greg MacDougall,[3] Graeme M. Luke,[3] Vladimir K. Michaelis,[4] Scott Kroeker,[4] Chris R. Wiebe,[5,6] Haidong Zhou,[5,6] and Lachlan M. D. Cranswick[7]

[1]*Department of Chemistry, McMaster University, Hamilton, Ontario, Canada L8S 4M1*

[2]*Brockhouse Institute for Materials Research, McMaster University, Hamilton, Ontario, Canada L8S 4M1*

[3]*Department of Physics and Astronomy, McMaster University, Hamilton, Ontario, Canada L8S 4M1*

[4]*Department of Chemistry, University of Manitoba, Winnipeg, Manitoba, Canada R3T 2N2*

[5]*Department of Physics, Florida State University, Tallahassee, 32310-4005 Florida, USA*

[6]*Department of Chemistry, University of Winnipeg, Winnipeg, Manitoba, Canada R3B 2E9*

[7]*Canadian Neutron Beam Centre, National Research Council, Chalk River Laboratories, Chalk River, Ontario, Canada K0J 1J0*

(Received 12 November 2009; revised manuscript received 4 January 2010; published 26 February 2010)

Two B-site ordered double perovskites, La_2LiReO_6 and Ba_2YReO_6, with $S=1$ were investigated as geometrically frustrated antiferromagnets, using x-ray and neutron diffraction, superconducting quantum interference device magnetometry, heat capacity, muon spin relaxation (μSR), and ^{89}Y magic-angle spinning (MAS) NMR. La_2LiReO_6 has a monoclinic structure ($P2_1/n$) with cell parameters at room temperature; $a=5.58262(22)$ Å, $b=5.67582(20)$ Å, $c=7.88586(27)$ Å, and $\beta=90.240(4)°$. A zero-field cooled/field cooled (ZFC/FC) divergence at 50 K was observed in the susceptibility. The ZFC susceptibility is zero below ~5 K for polycrystalline samples, suggesting a cooperative singlet ground state but weak moments are induced by cooling in very small fields ~1 mT. No evidence of long-range ordering is evident in heat capacity, neutron-diffraction, or μSR data. The ZF spin dynamics from μSR are anomalous and can be fitted to a stretched exponential rather than the Kubo-Toyabe form expected for random frozen spins but the muon spins are decoupled in longitudinal fields (LF), consistent with spin freezing of the fraction of spins relaxing within the muon time scale. The internal fields sensed by the muons are anomalously small, consistent with an electronic spin-singlet state. Ba_2YReO_6 is found to be cubic (Fm3m) with cell parameter $a=8.36278(2)$ Å at 300 K with no change in symmetry at 3.8 K, at variance with the Jahn-Teller theorem for a t_{2g}^2 configuration for Re^{5+}. ^{89}Y MAS NMR shows a single peak indicating that Y/Re site disorder is at most 0.5%. The susceptibility shows two broad peaks around 50 and 25 K but no evidence for long-range order from heat capacity, neutron diffraction, or μSR. The ZF μSR result shows a two-component ground state with both slow and fast relaxations and decoupling results in a 1 kG LF, indicating spin freezing. These results are in sharp contrast to the long-range AF order found in the $S=3/2$ isostructural materials, La_2LiRuO_6 and Ba_2YRuO_6, indicating that the reduction to $S=1$ plays a major role in ground state determination.

DOI: 10.1103/PhysRevB.81.064436 PACS number(s): 75.50.Lk, 75.50.Ee, 76.60.−k, 61.05.F−

I. INTRODUCTION

Geometrically frustrated antiferromagnetic materials have attracted considerable interest over the past few years, motivated by their tendency to form rather exotic magnetic ground states such as the spin glass, spin liquid, or spin ice states instead of long-range order in apparent defiance of the third law of thermodynamics.[1] Among the four "canonical" geometrically frustrated lattices: triangular planar, kagome, pyrochlore, and face-centered cubic (fcc), the latter has received the least attention. In real materials the fcc magnetic lattice is conveniently realized in the B-site ordered double perovskites, $A_2BB'O_6$. Here a magnetic ion resides on the B′ site, while B and A are nonmagnetic. Both the B and B′ sites constitute interpenetrating face-centered cubic sublattices, Fig. 1, which, if the exchange constraint between nearest B′ neighbors is antiferromagnetic, the basic criteria for geometric frustration are satisfied. The conditions for B-B′ site ordering have been presented in the form of a phase diagram.[2]

A very important feature of B-site ordered double perovskites is the versatility of this structure type to chemical substitution. The large A-site ions are generally from Group II or III and the B and B′ ions from the transition series 3*d*-5*d* and 4*f* or small Group I, II, or III ions. The crystal symmetry can be tuned via the familiar tolerance factor, *t*, which for double perovskites can be written

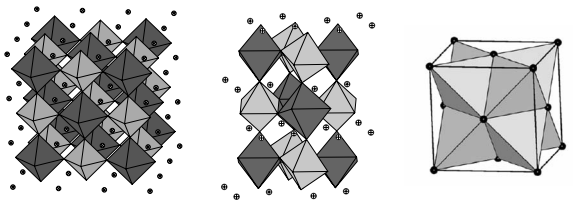

FIG. 1. (Left) Cubic (Fm3m) structure of the B-site ordered double perovskite $A_2BB'O_6$. Dark gray octahedra represent $B'O_6$ and light gray octahedra represent BO_6. The small spheres represent the A ions. (Center) The monoclinic ($P2_1/n$) structure with the same shading scheme. (Right) The face-centered cubic lattice of B′ sites which is geometrically frustrated.

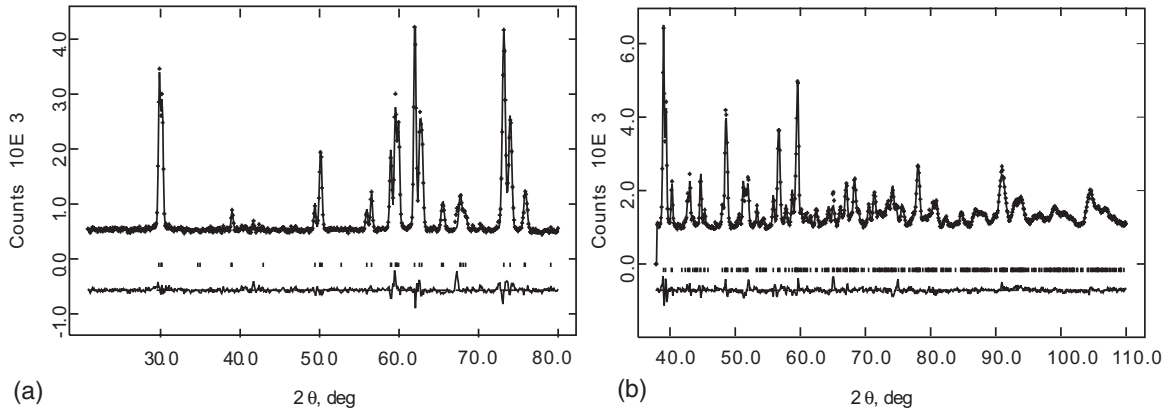

FIG. 2. A Rietveld fit to the neutron-diffraction data for La_2LiReO_6 for two wavelengths, $\lambda = 2.37192$ Å (a) and $\lambda = 1.33052$ Å (b) at 298 K.

$$t = (r_A + r_O)/2^{1/2}(r_{\langle B,B'\rangle} + r_O),$$

where $r_{\langle B,B'\rangle}$ is the average of the B and B′ ionic radii, r_A is the radius of A and r_O that of the oxide ion. For $t \sim 1$ one finds Fm3m crystal symmetry and cubic, m3m, point symmetry at the B sites. As t decreases, the crystal symmetry descends and one commonly finds materials with I4/m(4/m), $P2_1/n(-1)$, and P-1(−1) space groups and corresponding point-group symmetries at the B′ site indicated in parentheses.[3]

Thus, the B-site ordered double perovskites provide an unique opportunity for a systematic study of the roles of several factors, including the spin quantum number, S, and the local site symmetry on the nature of the magnetic ground state in the frustrated fcc lattice. In a previous paper the $S = 3/2$ materials Ba_2YRuO_6 (Fm3m) and La_2LiRuO_6 ($P2_1/n$) were reinvestigated in detail. While both show behavior typical of geometrically frustrated materials, long-range AF order is found in both below 36 and 24 K, respectively.[4] In this work the systematic study is extended to the $S = 1$ materials La_2LiReO_6 and Ba_2YReO_6. For the former only a crystal structure has been reported while the latter has been investigated using x-ray diffraction, magnetic susceptibility, and heat capacity.[5,6] For both materials the crystal structure is reinvestigated using neutron diffraction, which resulted in new assignments of crystallographic symmetry, along with ^{89}Y magic-angle spinning (MAS) NMR to test Y/Re ordering in Ba_2YReO_6. In addition to superconducting quantum interference device (SQUID) magnetometry and heat capacity, the spin dynamics has been studied using muon spin relaxation (μSR). It is demonstrated that these $S = 1$ compounds do not show long-range order to 2 K, unlike the $S = 3/2$ analogs but instead anomalous spin freezing (Ba_2YReO_6) and the formation of a cooperative spin-singlet state with a finite concentration of defects (La_2LiReO_6).

II. EXPERIMENTAL PROCEDURES

La_2LiReO_6 was prepared using a conventional solid-state reaction. A mixture of La_2O_3 (Aldrich, 99.9%, preheated to

TABLE I. The refined cell parameters and atomic positions of La_2LiReO_6 from neutron powder data at 298 and 2.8 K.

	298 K				2.8 K			
Atom	x	y	z	U_{iso} (Å^2)	x	y	z	U_{iso} (Å^2)
La	−0.0104(8)	0.0476(5)	0.2525(6)	0.0095(8)	−0.0117(9)	0.0493(7)	0.2559(6)	0.0033(12)
Li	0.5	0	0	0.017(5)	0.5	0	0	0.001(6)
Re	0.5	0	0.5	0.0059(9)	0.5	0	0.5	0.0034(14)
O1	0.1936(10)	0.2192(10)	0.0446(8)	0.0105(18)	0.1926(12)	0.2187(11)	−0.0474(9)	0.0065(24)
O2	0.2828(10)	0.3048(11)	0.0414(9)	0.0143(17)	0.2869(12)	0.3042(11)	0.0405(10)	0.0058(21)
O3	0.0830(9)	−0.5192(8)	0.2395(7)	0.0107(13)	0.0823(11)	0.5216(11)	0.2399(8)	0.0091(20)
a	5.58262(22)				5.58070(31)			
b	5.67582(20)				5.68591(28)			
c	7.88586(27)				7.8405(4)			
β	90.240(4)				90.464(5)			
χ^2	1.71				2.61			
R_p	0.0367				0.0443			
R_{wp}	0.0505				0.0635			

TABLE II. Selected bond distances (Å) and angles (°) for La_2LiReO_6 at 298 and 2.8 K.

Bond length (Å)	2.8 K	298 K
Li-O1	2.149(6)	2.143(5)
Li-O2	2.122(6)	2.137(5)
Li-O3	2.097(6)	2.110(5)
Re-O1	1.964(6)	1.959(5)
Re-O2	1.978(6)	1.957(6)
Re-O3	1.937(6)	1.946(5)
Bond angles (deg)	**2.8 K**	**298 K**
Li-O1-Re	151.1(4)	152.1(4)
Li-O2-Re	152.7(4)	152.9(4)
Li-O3-Re	152.7(4)	152.82(29)

remove moisture and surface contamination), 10% excess of Li_2CO_3 (J.T. Baker Chemical Co., 99.1%), Re (Alfa Aesar, 99.997%), and ReO_3 (Rhenium Alloys Inc.) was ground and heated in an Ar flow in two stages, first to 923 K at 100°/h and held for 6 h, then fired at 1173 K for 10 h. For Ba_2YReO_6, a stoichiometric mixture of starting reagents, $BaCO_3$ (J.T. Baker Chemical Co.), Y_2O_3 (Alfa Aesar, 99.9%, preheated), Re (Alfa Aesar, 99.997%), and ReO_3 (Rhenium Alloys Inc.) was ground and heated in an Ar flow again in two stages, first at 1143 K for 6 h and then at 1573 K for 24 h. A second firing at 1573 K for 24 h was required for completion of the reaction. The obtained powders were black and the sample purity was tested by x-ray diffraction using a Gunier-Hägg camera with Cu $K\alpha_1$ radiation.

Magnetic-susceptibility measurements were performed with applied fields of 10, 100, and 5000 Oe at McMaster University using a Quantum Design MPMS SQUID magnetometer. Zero-field cooling (ZFC) and field cooling (FC) data were collected in the temperature range of 2 to 300 K. A hysteresis measurement for La_2LiReO_6 was performed at 5 K with an applied field range between -5.5 T and 5.5 T.

Heat-capacity measurements were carried out at McMaster using an Oxford Maglab and at Florida State University/

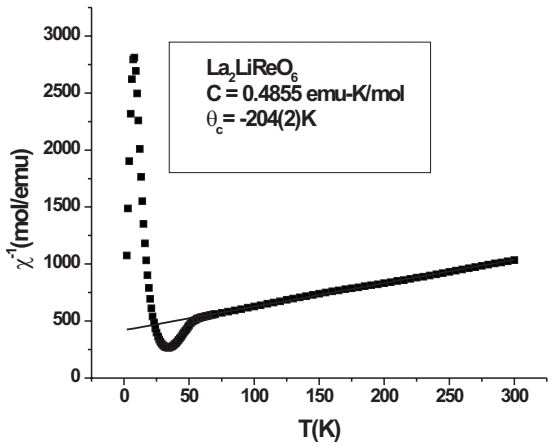

FIG. 3. Inverse susceptibility for La_2LiReO_6 showing the Curie-Weiss fit.

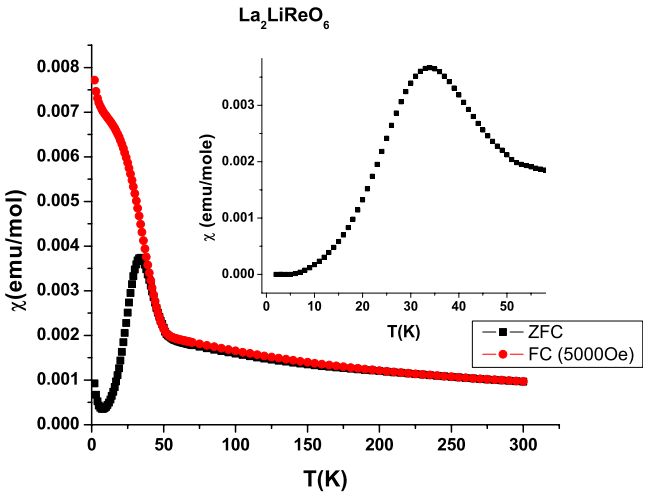

FIG. 4. (Color online) Temperature dependence of the susceptibility of La_2LiReO_6 at an applied field of 0.5 T. The inset shows the result of subtracting the weak Curie tail and evidence for a magnetic singlet ground state.

NHMFL using a Quantum Design PPMS system in the temperature range of 2 to 70 K. Lattice match compounds, La_2LiIrO_6 and Ba_2YTaO_6 (Refs. 7 and 8) were prepared according to literature methods and measured to estimate the lattice heat-capacity contribution for La_2LiReO_6 and Ba_2YReO_6.

Neutron-diffraction measurements were performed on the C2 diffractometer at the Canadian Neutron Beam Centre operated by the National Research Council of Canada at the Chalk River laboratories of Atomic Energy of Canada. The data were collected at room temperature and 2.8 K with neutron wavelengths of 2.7319 and 1.3305 Å for La_2LiReO_6 and at 4, 10, 20, 40, and 300 K with neutron wavelengths of 2.36927 and 1.3286 Å for Ba_2YReO_6. The crystal structures of both compounds were refined using FULLPROF (Ref. 9) or GSAS.[10]

Local spin dynamics were investigated using ZF and longitudinal field (LF) μSR at TRIUMF, Vancouver, Canada. The measurement temperatures were 2 K and 10 K–60 K in 10 K increments in ZF μSR and 2 K with applied fields of 100 and 500 G in LF μSR for La_2LiReO_6. For Ba_2YReO_6, the measurement temperatures were at 2, 5, 15, 25, 35, 40,

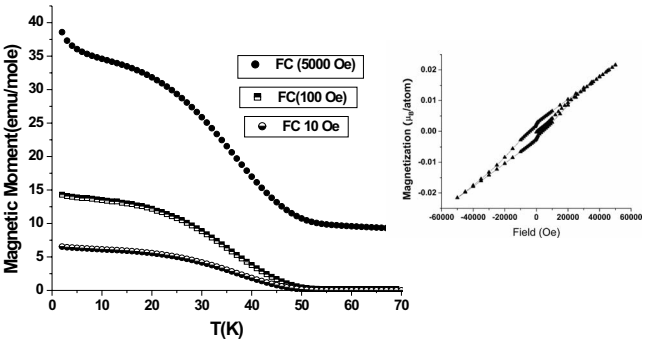

FIG. 5. Temperature dependence of the FC susceptibility showing onset of a very weak moment below 50 K for all applied fields. The inset shows hysteresis at 5 K.

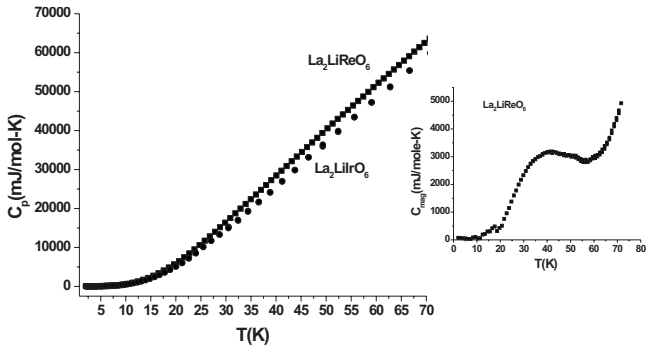

FIG. 6. The heat capacity of La_2LiReO_6 and the lattice match sample, La_2LiIrO_6. The inset shows the magnetic component and a very broad maximum between 40–50 K.

42.5, 50, 55, and 100 K in ZF μSR and 2 K with an applied field of 1 kG in LF μSR. ^{89}Y MAS solid-state NMR was performed on Ba_2YReO_6 in the Department of Chemistry at the University of Manitoba. The spectrum was collected on a 3.2 mm double-resonance Varian-Chemagnetics MAS probe using a Bloch-decay pulse sequence on a Varian Inova$^{\text{UNITY}}$ 600 (14.1 T) spectrometer operating at a Larmor frequency, ν_L of 29.36 MHz. The sample (black crushed powder) was packed into a 3.2 mm (o.d.) ZrO_2 rotor with a fill volume of 22 μL and spun at 22.000 ± 0.015 kHz. The spectrum is the result of 785 408 coadded transients, acquired with a 45° tip angle (ν_{rf}=45 kHz) and a recycle delay of 400 ms. The sample temperature was maintained at 303 K, and the chemical shift was referenced with respect to external 2 M $Y(NO_3)_3$ at 0.0 ppm.[11]

III. RESULT AND DISCUSSION

A. La_2LiReO_6

1. Crystal structure

The obtained powder was confirmed to be single phase by x-ray diffraction. The crystal structure of this compound is shown in Fig. 1. This compound was first reported to have an orthorhombic structure with cell parameters a=5.577 (Å), b=5.663 (Å), and c=7.876 (Å) from x-ray powder diffraction.[5] On the contrary, two related compounds

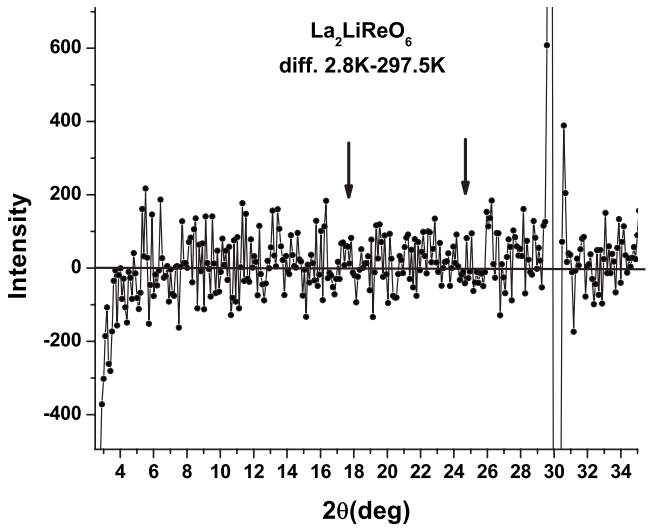

FIG. 7. A low-angle neutron-diffraction difference plot 2.8–297.5 K showing the absence of magnetic Bragg peaks. The arrows show the location of expected reflections for a type I fcc structure as found for La_2LiRuO_6 (Ref. 4).

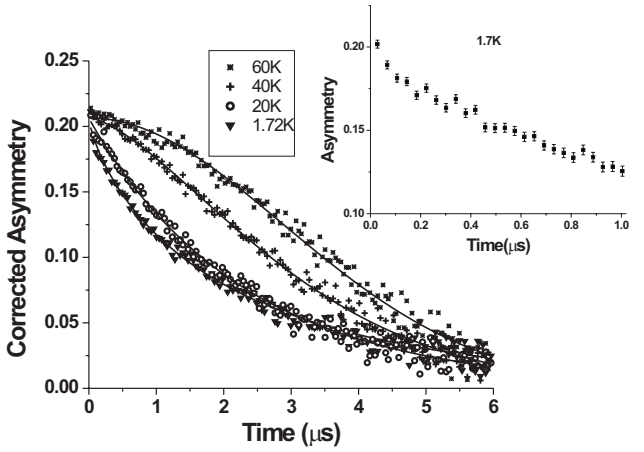

FIG. 8. Fit of the slowly relaxing component, $t>0.02$ μs to a stretched exponential. The inset shows the weak, rapidly relaxing component for $t<0.1$ μs which develops below 20 K. Only the 1.7 K data are shown.

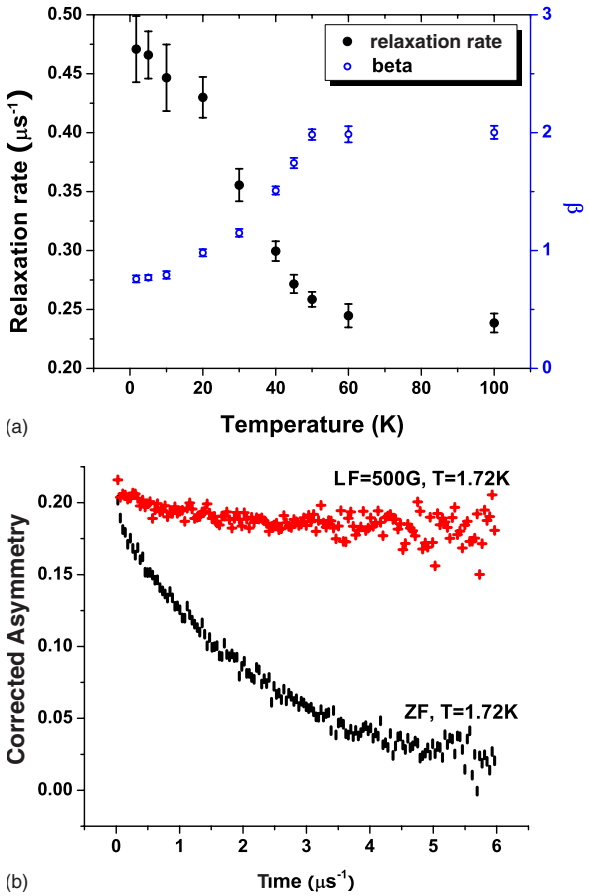

FIG. 9. (Color online) (a) Temperature dependence of the relaxation rate and the exponent, β, extracted from the fit to a stretched exponential function for the data of Fig. 8. (b) Application of a 500 Oe LF (upper curve) for La_2LiReO_6 showing decoupling of both components at 1.7 K.

TABLE III. The refined cell parameters and atomic positions of Ba_2YReO_6 from neutron powder data.

	4 K				300 K			
Atom	x	y	z	B_{iso} (Å^2)	x	y	z	B_{iso} (Å^2)
Ba	0.25	0.25	0.25	0.44(2)	0.25	0.25	0.25	0.91(2)
Y	0.5	0.5	0.5	0.68(4)	0.5	0.5	0.5	1.01(5)
Re	0	0	0	0.14(3)	0	0	0	0.23(3)
O	0.23396(14)	0	0	0.66(1)	0.22380(16)	0	0	1.09(2)
a	8.3395(2)				8.3627(2)			
χ^2	5.32				5.83			
R_p	5.42				5.05			
R_{wp}	7.31				6.91			

La_2LiRuO_6 (Refs. 4 and 12) and La_2LiMoO_6,[13] have been reported as monoclinic, $P2_1/n$, from neutron powder or single-crystal x-ray diffraction. From Shannon's ionic radii Re^{5+} resides between Mo^{5+} and Ru^{5+} [Mo^{5+}=0.61 Å, Re^{5+}=0.58 Å, and Ru^{5+}=0.565 Å (Ref. 14)], therefore, it is highly likely that La_2LiReO_6 is monoclinic as well. Thus, the neutron-diffraction data collected at 2.8 and 298 K were refined in $P2_1/n$, and the results are shown in Fig. 2 and Table I where the fit is seen to be excellent with a β angle significantly greater than 90.00(deg). Examination of the interatomic distances, Table II, indicates that the nearest-neighbor coordination environment of Re shows a weak pseudotetragonal compression at 298 K which is enhanced somewhat at 2.8 K.

2. *Magnetic properties*

First, the inverse susceptibility, Fig. 3, was fitted to the Curie-Weiss law for the range 100–300 K, yielding a Weiss temperature, θ=−204(2) K, and an effective magnetic moment of $1.97\mu_B$, which is smaller than the spin-only value ($2.82\mu_B$) for a S=1 ion.

The large, negative, θ indicates predominant antiferromagnetic exchange and the magnitude is somewhat larger than for the S=3/2 analog, La_2LiRuO_6 (−185 K).[4,12] This indicates, given the smaller S value, even stronger overall AF exchange for the Re compound. The magnetic susceptibility at low temperatures is shown in Fig. 4 at an applied field of 0.5 T. Note the ZFC/FC divergence below ~50 K. The ZFC curve shows a broad maximum at 33 K but this shifts to higher temperatures for smaller fields (1 and 10 mT—data not shown). Note that the ZFC susceptibility at an applied field of 0.5 T approaches zero at low temperatures. This is shown more clearly in the inset to Fig. 4 where the low-temperature Curie-Weiss tail has been subtracted. Such behavior is remarkable for a polycrystalline sample and is consistent with a spin-singlet ground state. The FC susceptibility shows that a very weak moment is induced below 50 K regardless of applied field, Fig. 5, and that hysteresis is found at 5 K with induced moments on the order of $10^{-2}\mu_B$ per Re ion (inset). The observation of ZFC/FC divergences and hysteresis indicates that the singlet state is collective and not single ion in nature. The most consistent interpretation of the bulk susceptibility is that a collective spin-singlet state is the ground state but that a low concentration of nonsinglet defects can be induced with even very low fields. The presence or absence of a spin gap in this material is unclear at this time. Further studies including inelastic neutron scattering and Li NMR are planned to investigate this possibility.

To search for evidence for or against long-range magnetic order heat-capacity data were collected over the range including the ZFC/FC divergence and below, and no lambda anomaly is seen, Fig. 6. Note that the data are superimposed on those for the lattice match material below about 10 K, which suggests no electronic contribution. The magnetic component shows a very broad maximum between 40–50 K, consistent with the bulk susceptibility. Entropy removal within the temperature range studied is 3.5 J/mol K^2 which is ~38% of the total entropy expected for a S=1 system.

As well, a difference plot of the neutron-diffraction data for 2.8 and 298 K was examined for magnetic Bragg peaks with negative results, Fig. 7. Such features were easily seen for the isostructural, S=3/2 analog, La_2LiRuO_6.[12] Given the difference in spin quantum number, one would expect corresponding magnetic Bragg peaks for the Re compound to be reduced in intensity by a factor of ~2. Assuming the same magnetic structure, such reflections should have been detected and they are clearly absent. Thus, both heat-capacity and neutron-diffraction data support the absence of long-range magnetic order in La_2LiReO_6.

To investigate the local spin dynamics, μSR measurements were performed. The corrected data for ZF μSR at 60 K (paramagnetic), 40 K (just below the ZFC/FC divergence), 20 and 1.7 K are shown in Fig. 8. Below 20 K (inset) there are clearly two components, one rapidly relaxing in the region <0.1 μs, and one slowly relaxing which extends to several microseconds. It proved impossible to fit the all of the data to a two-component relaxation function including the fast component, so the data for the slow component only

TABLE IV. Selected interatomic distances (Å) for Ba_2YReO_6 at 300 and 4 K.

Bond length (Å)	4 K	300 K
Y-O	2.2186(1)	2.2262(1)
Re-O	1.9512(1)	1.9552(13)

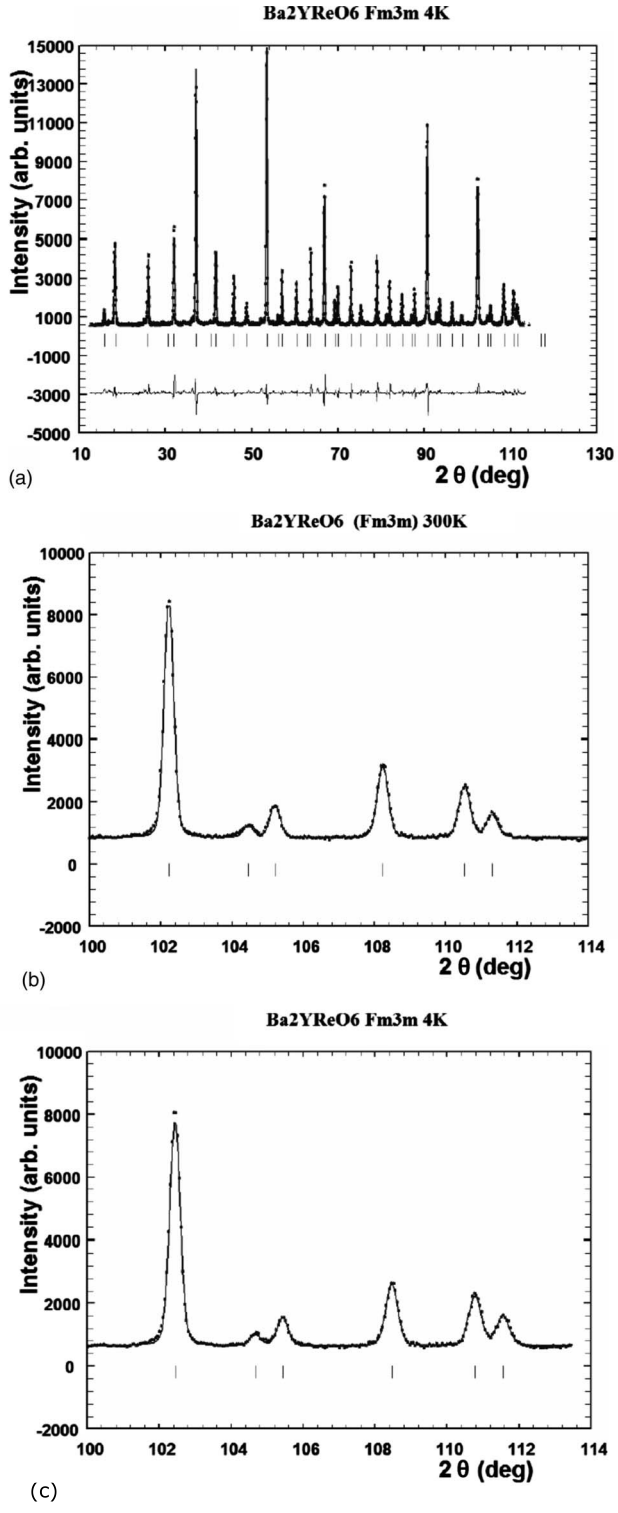

FIG. 10. (a) Neutron-diffraction pattern and the refinement for Ba_2YReO_6 at 4 K. (b) High-angle, high-resolution ($\Delta d/d \sim 2 \times 10^{-3}$) neutron-diffraction data at 4 K and (c) 300 K showing no distortion from cubic symmetry.

were fitted, shown as the solid line, with a stretched exponential, $A(t)=A_0^* \exp[-(\lambda t)^\beta]$, where A is an amplitude and λ is a relaxation rate. The temperature dependence of the extracted relaxation rate is shown in Fig. 9(a) along with the

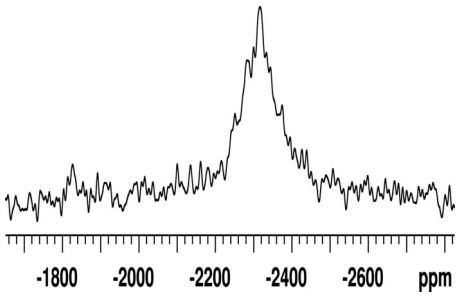

FIG. 11. ^{89}Y MAS NMR of Ba_2YReO_6 acquired at 22 kHz. The center of gravity chemical shift is −2320(15) ppm with a width of 90 ppm. The apparent peak at ~−1820 ppm is an experimental artifact from the transmitter.

behavior of the exponent, β. The rate is roughly constant until ~50 K (the ZFC/FC divergence temperature) and then increases gradually, reaching a saturation value only below ~20 K consistent with some level of spin freezing. The β value remains constant at ~2 down to 50 K, consistent with paramagnetic relaxation, then decreases sharply, indicating that electron spins are involved. In contrast to other Re-based double perovskites with $S=1/2$ such as Sr_2CaReO_6 or Sr_2MgReO_6,[15,16] the relaxation data do not exhibit the classic Kubo-Toyabe line shape often found for frozen spin ground-state materials in which essentially all of the spins freeze. Instead, the observed stretched exponential decay is typical of dilute spin systems, which is curious as the concentration of magnetic Re^{5+} ions is nominally high in this material. Application of a 500 Oe LF, Fig. 9(b), decouples the muons at 2 K, indicating that the electron spins, which couple to the muons, are static at this temperature. The very slow relaxation of the muons in La_2LiReO_6 indicates coupling to very weak electronic fields, which is consistent with the singlet ground-state behavior seen in the bulk susceptibility, if it is postulated that most of the Re spins are involved in the singlet state, leaving only a remnant fraction to couple with the muon spins. It is worth noting that the weak local fields cannot be due to some type of symmetry cancellation in this system as the muon will be hydrogen bonded to the O atoms

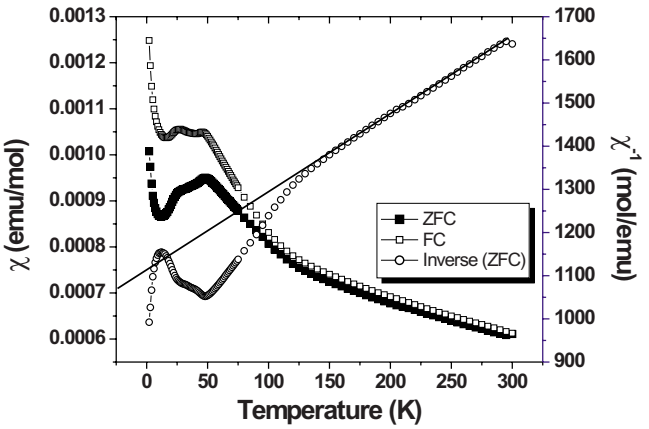

FIG. 12. (Color online) The magnetic susceptibility of Ba_2YReO_6. A Curie-Weiss fit of the inverse susceptibility data, solid line, yields the parameters $C=0.554(5)$ (emu/mole K) and $\theta=-616(7)$ K.

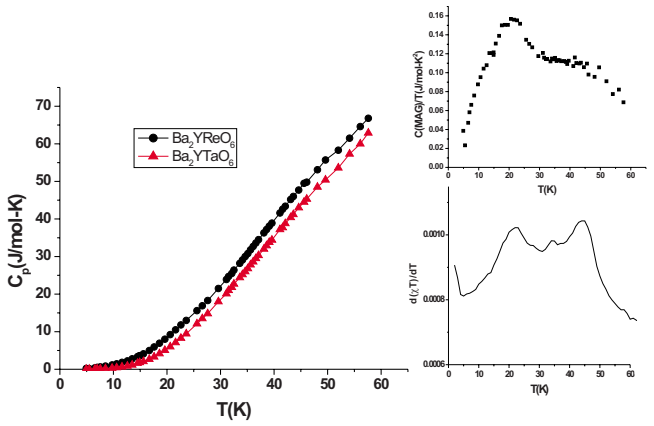

FIG. 13. (Color online) Heat capacity of Ba_2YReO_6 and Ba_2YTaO_6. The insets show: (top) the magnetic component plotted as $C_{(MAG)}/T$ vs T. (Bottom) Fisher's heat capacity, $d(\chi T)/dT$ vs T (Ref. 18).

which are in sites of very low crystallographic symmetry.

B. Ba_2YReO_6

1. Crystal structure

This compound was previously studied by Sasaki *et al.*[6] and reported to be monoclinic, $P2_1/n$ by the refinement of a powder x-ray diffraction data collected at room temperature. Examination of the results from this study revealed that the monoclinic cell constants were metrically cubic to within experimental error. Thus, the neutron-diffraction data obtained here were refined in Fm3m. The results, given in Fig. 10(a) and Tables III and IV, show that the choice of Fm3m is correct. As seen in Fig. 10(b), there is no detectable distortion from cubic symmetry at 300 or 3.5 K within the resolution of the neutron data which is $\Delta d/d \sim 2 \times 10^{-3}$ for the 2θ range covered in the figure. This result is of considerable interest as Re^{5+}, $5d^2$ has the t_{2g}^2 configuration in cubic symmetry and is thus subject to the Jahn-Teller theorem and some distortion would be expected.

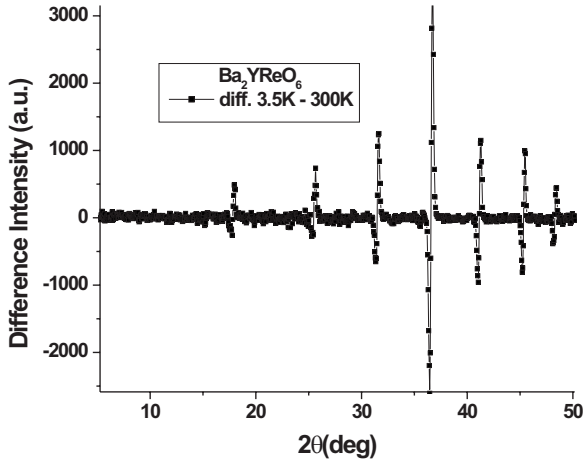

FIG. 14. The difference neutron-diffraction pattern, 3.5–300 K for Ba_2YReO_6, showing the absence of detectable magnetic Bragg peaks.

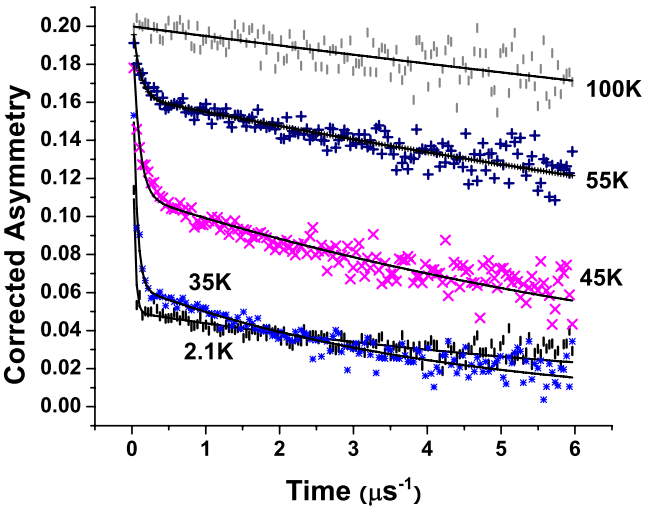

FIG. 15. (Color online) ZF-μSR relaxation data at selected temperatures for Ba_2YReO_6. The fitted lines are to a sum of two exponential decay functions, see text.

In addition to the crystal structure, Y/Re ordering is an issue to be addressed since the charge difference of 2 and the ionic radii difference between Y^{3+} and Re^{5+} ions places this material near the border of the phase diagram of Anderson *et al.*[2] for B-site ordering in double perovskites. Thus, a ^{89}Y MAS NMR measurement was carried out to investigate the level of Y/Re ordering. Previously, the same technique disclosed a 1% site mixing between Y and Ru in isostructural Ba_2YRuO_6.[4] As shown in Fig. 11, a single peak is observed at −2320 ppm with a peak width [full width at half maximum (FWHM=2.55 kHz)] comparable to that in Ba_2YRuO_6.[4] No additional signals could be detected over a 6000 ppm range. It may be noted that the peak position is midway between the "normal" ^{89}Y chemical shielding range and the approximately −5800 ppm positions observed for the $S=3/2$ Ba_2YRuO_6, evidence that interaction with the unpaired electron spins dominates the nuclear shielding properties. From these results it can be concluded that there is no convincing evidence for Y/Re site disorder in Ba_2YReO_6. Using the arguments of Refs. 4 and 17 an upper limit of Y/Re disorder is generously estimated to be 0.5%.

2. Magnetic properties

The magnetic susceptibility for Ba_2YReO_6 is displayed in Fig. 12. It shows two broad maxima at 50 and 25 K, which is consistent with the data previously reported by Sasaki *et al.*[6] although their results do not show the 25 K anomaly so clearly. The ZFC/FC curves show a slight divergence around 125 K. The inverse susceptibility was fitted with the Curie-Weiss law yielding a Weiss temperature, $\theta=-616(7)$ K and an effective magnetic moment, $\mu_{eff}=1.93\mu_B$. This reduced effective moment compared to its spin only value ($2.83\mu_B$) may be due to orbital contributions. The reported Weiss temperature ($\theta=-723$ K) of Sasaki *et al.* is somewhat larger than that seen here, which could result from a different choice of the temperature region for the fitting. The frustration index derived here is $f \sim 15$.

Previous heat-capacity data from Sasaki *et al.*[6] showed the absence of any lambda peak, which would signal long-range magnetic order. The data of Fig. 13 show the heat capacity of Ba_2YReO_6 compared with a lattice match material, Ba_2YTaO_6. In the inset is plotted the magnetic component, as C_{MAG}/T vs T. Two broad anomalies near 25 and 50 K are evident as is the absence of a sharp lambda peak. Also shown is the Fisher heat capacity, $d(\chi T)/dT$ vs T, derived from the susceptibility data.[18] The total entropy removed below 60 K is 5.79 J/mol K^2, 63% of that expected for $S=1$.

In order to clarify further the ground state of this compound, we have conducted neutron-diffraction measurements and muon spin relaxation measurements. The difference neutron-diffraction data, 4–300 K, are shown in Fig. 14. Magnetic Bragg peaks are absent, providing evidence against long-range order.

The μSR relaxation data for Ba_2YReO_6 are shown in Fig. 15. Data at 100 K show paramagnetic behavior, but the line shape is clearly non-Gaussian indicating that the relaxation is due to coupling to electron spins. As the temperature decreases, two components develop, a fast relaxing one at short t due to quasistatic internal fields and a slowly relaxing one extending to long t. Fitting over the entire t range was done with the equation, $F(t)=A^*_{fast}\exp(-\lambda^*_{fast}t)+A^*_{slow}\exp(-\lambda^*_{slow}t)$ and the extracted amplitudes and frequencies for the two components are shown versus temperature in Fig. 16. From the amplitudes, Fig. 16(a), the fast component builds gradually until ~40 K and saturates below ~30 K at ~3/4 of the total spins while the slow tail amplitude decreases gradually and also saturates below 30 K at ~1/4 of the total spins. The observation of two spin components for this material is puzzling as there is only one crystallographic oxygen site, and thus, normally, one muon site. More remarkably, the rates for the two components show very different temperature dependencies, Fig. 16(b). The slow component peaks at ~35 K, just below the higher temperature feature in the susceptibility and heat-capacity data, which suggests that this is the spin freezing temperature. The fast component shows no peak but saturates below 20 K, near the lower temperature feature in the bulk susceptibility and heat capacity.

According to the LF-μSR data collected at 2.1 K, Fig. 17, all of the spins are decoupled with an applied field of 1 kG, therefore, both components show spin freezing. Nonetheless, the ground state is clearly inhomogeneous compared to more conventional spin glasses which usually follow the Kubo-Toyabe model in ZF wherein the amplitude fractions of the fast and slow components are 2/3 and 1/3, respectively, and are not generally strongly temperature dependent within the frozen spin regime. Thus, Ba_2YReO_6 shows a somewhat more conventional frozen spin ground state rather than the exotic singlet state found for La_2LiReO_6. Nonetheless, chemical disorder in this material is below the detection limits of either neutron diffraction or ^{89}Y MAS NMR. Thus, the origin of the spin frozen state is unclear at this time. It is important to recall that a detectable level of site disorder, ~1–2%, was found in the $S=3/2$ analog, Ba_2YRuO_6 which was insufficient to destroy long-range AF order.[4]

IV. SUMMARY AND CONCLUSIONS

The structure and magnetic properties of the B-site ordered double perovskites La_2LiReO_6 and Ba_2YReO_6, in

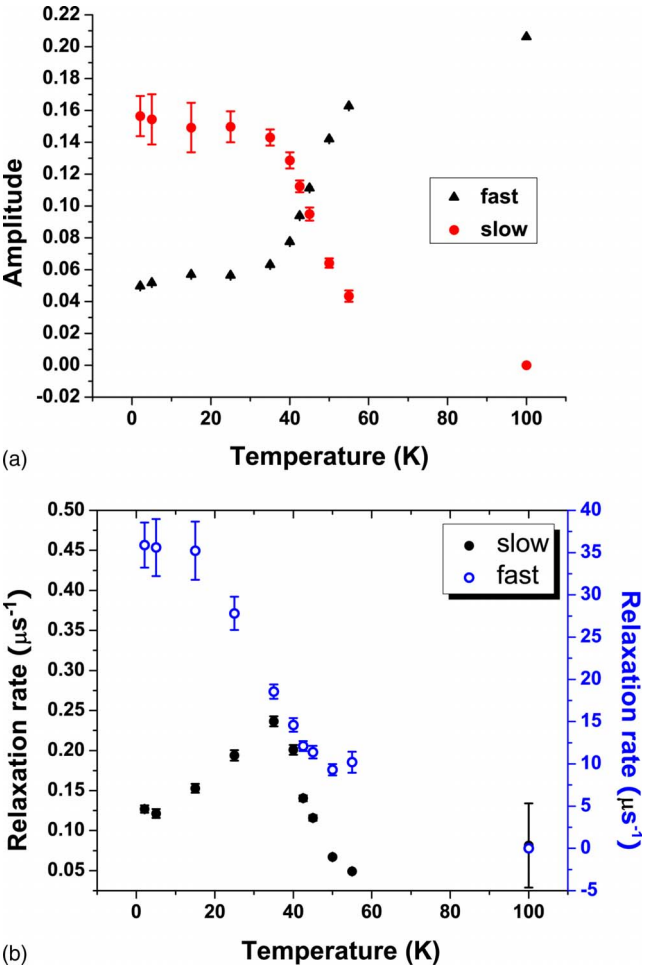

FIG. 16. (Color online) (a) The temperature dependence of the amplitudes of the fast and slow components in μSR for Ba_2YReO_6. (b) The temperature dependences of the relaxation rates of the slow and fast components.

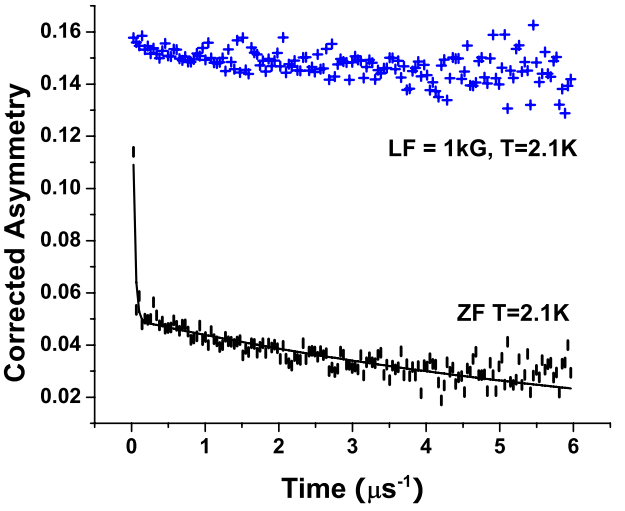

FIG. 17. (Color online) μSR relaxation for Ba_2YReO_6 in a LF of 1 kG at 2.1 K, showing complete decoupling, an indication of static spins.

which the $S=1$ ion, Re^{5+}, resides on a fcc lattice were investigated from the perspective of geometric magnetic frustration. The crystal structures are different from previous reports, monoclinic ($P2_1/n$) rather than orthorhombic for La_2LiReO_6, and cubic ($Fm3m$) rather than monoclinic for Ba_2YReO_6 but consistent with those of compositionally similar materials. The latter shows no detectable Y/Re disorder using the very sensitive probe of ^{89}Y MAS NMR. No long-range order was found to 2 K from SQUID magnetometry, heat capacity, neutron diffraction, and μSR for either material. For La_2LiReO_6 bulk susceptibility, heat capacity, and μSR data point toward a collective spin-singlet ground state, which must involve a finite defect concentration, as weak spontaneous moments are induced by cooling in small fields. Ba_2YReO_6 shows somewhat more conventional behavior leading to a frozen spin ground state but without an obvious source of positional disorder. It is clear that long-range order is quenched for both cubic and monoclinic symmetries for these $S=1$ double perovskites in contrast to their $S=3/2$ analogs, Ba_2YRuO_6 and La_2LiRuO_6, which show evidence for strong geometric frustration but which ultimately undergo AF long-range order.[4] Of equal interest is the striking difference in behavior of the two $S=1$, Re^{5+} double perovskites. The most obvious electronic difference between the two materials would appear to be the orbital degeneracy. The t_{2g}^2 configuration is retained in cubic Ba_2YReO_6, which implies an orbital liquid, while an orbital singlet state should exist for monoclinic La_2LiReO_6. The evidence for a collective spin-singlet ground state for the latter is remarkable and unexpected for a $S=1$ system. Clearly, much further work, both experiment and theory, is needed for a more complete understanding of these results.

ACKNOWLEDGMENTS

We thank Paul Dube for assistance with SQUID and heat-capacity measurements. J.E.G, G.M.L., V.K.M., and S.K. thank NSERC. S.K. thanks the Canada Foundation for Innovation and G.M.L. thanks the Canadian Institute for Advanced Research. For work done at Florida State University, C.R.W. thanks the NSF for funding through Grant No. DMR-08-04173. We appreciate the technical support of the TRIUMF Center for Materials and Molecular Science and the Canadian Neutron Beam Centre.

[1] A. P. Ramirez, Annu. Rev. Mater. Sci. **24**, 453 (1994); J. E. Greedan, J. Mater. Chem. **11**, 37 (2001).
[2] M. T. Anderson, K. B. Greenwood, G. A. Taylor, and K. R. Poppelmeier, Prog. Solid State Chem. **22**, 197 (1993).
[3] C. J. Howard, B. J. Kennedy, and P. M. Woodward, Acta Crystallogr., Sect. B: Struct. Sci. **59**, 463 (2003).
[4] T. Aharen, J. E. Greedan, F. Ning, T. Imai, V. K. Michaelis, S. Kroeker, H. Zhou, C. R. Wiebe, and L. M. D. Cranswick, Phys. Rev. B **80**, 134423 (2009).
[5] K. Hayashi, H. Noguchi, and M. Ishii, Mater. Res. Bull. **21**, 401 (1986).
[6] Y. Sasaki, Y. Doi, and Y. Hinatsu, J. Mater. Chem. **12**, 2361 (2002).
[7] K. Hayashi, G. Demazeau, M. Pouchard, and P. Hagenmuller, Mater. Res. Bull. **15**, 461 (1980); J. Darriet, G. Demazeau, and M. Pouchard, *ibid.* **16**, 1013 (1981).
[8] P. J. Saines, J. R. Spencer, B. J. Kennedy, and M. Avdeev, J. Solid State Chem. **180**, 2991 (2007).
[9] J. Rodríguez-Carvajal, Physica B **192**, 55 (1993).
[10] B. H. Toby, J. Appl. Cryst. **34**, 210 (2001); A. C. Larson and R. B. Von Dreele, Los Alamos National Laboratory Report No. LAUR 86-748, 2004 (unpublished).
[11] K. J. D. MacKenzie and M. E. Smith, *Multinuclear Solid-State NMR of Inorganic Materials* (Pergamon, New York, 2002).
[12] P. D. Battle, C. P. Grey, M. Hervieu, C. Martin, C. A. Moore, and Y. Paik, J. Solid State Chem. **175**, 20 (2003).
[13] J. Tortelier and P. Gougeon, Acta Crystallogr., Sect. C: Cryst. Struct. Commun. **52**, 500 (1996).
[14] R. D. Shannon, Acta Crystallogr., Sect. A: Cryst. Phys., Diffr., Theor. Gen. Crystallogr. **32**, 751 (1976).
[15] C. R. Wiebe, J. E. Greedan, G. M. Luke, and J. S. Gardner, Phys. Rev. B **65**, 144413 (2002).
[16] C. R. Wiebe, J. E. Greedan, P. P. Kyriakou, G. M. Luke, J. S. Gardner, A. Fukaya, I. M. Gat-Malureanu, P. L. Russo, A. T. Savici, and Y. J. Uemura, Phys. Rev. B **68**, 134410 (2003).
[17] C. P. Grey, M. E. Smith, A. K. Cheetham, C. M. Dobson, and R. Dupre, J. Am. Chem. Soc. **112**, 4670 (1990).
[18] M. E. Fisher, Philos. Mag. **7**, 1731 (1962).